



Research article

Automated comet assay segmentation using combined dot enhancement filters and extended-maxima transform watershed segmentation

Lavdie Rada Ulgen^{*1} ¹ Bahcesehir University, Faculty of Engineering and Natural Sciences, Department of Mathematics, 34353, Istanbul, Türkiye

Abstract

The comet assay, also known as single-cell gel electrophoresis, is a widely used and reliable method for assessing DNA damage and repair in individual cells. It plays a crucial role in the assessment of genetic damage potential and human biomonitoring studies in the medical and biological fields. Ensemble of comet assay individual cells and establishing accurate information on the occurrence of cellular injury followed by the process of cellular restoration is a challenging task. This paper introduces an algorithm for the detection of a distinct head, composed of undamaged DNA, and a tail, comprising damaged or fragmented DNA, in genotoxicity testing images, and provides information on the region properties of such images. The proposed approach combines a dot enhancement filter to distinguish and help in the detection of the head in each cell combined with a multilevel segmentation approach consisting of a watershed-geodesic active contour model that is capable to refine the tail estimation. The effectiveness of the suggested algorithm is quantitatively evaluated with annotation data provided by biologists, and its results are compared with those obtained from previous works. The proposed system exhibits comparable or superior performance to the existing systems while avoiding excessive computational costs.

Keywords: Comet assay; dot enhancement filters; extended-maxima transform; image processing; segmentation; single cell gel; watershed

1. Introduction

DNA, the fundamental blueprint of life, contains all the necessary information for the construction and maintenance of our bodies. However, DNA is constantly subjected to various harmful factors that can lead to its degradation and result in genetic alterations (Chatterjee and Walker, 2017). To effectively study and understand these alterations, reliable techniques are needed to detect and quantify DNA damage at the level of individual cells. A notable method in biological research for evaluating DNA damage is the single-cell gel electrophoresis (SCGE) assay, commonly referred to as the comet assay (Singh et al., 1988; Uthirapathy, 2023). This technique provides a visual, sensitive, fast, and reliable approach to analyzing DNA damage, as introduced by Ostling and Johanson (1984). In this

method, individual cells are embedded in a thin agarose gel on a microscope slide as explained by Fairbairn et al. (1995). The resulting image resembles a comet, with a distinct head composed of intact DNA and a tail consisting of damaged or broken DNA fragments (Fig. 1). The extent of DNA released from the comet's head during electrophoresis correlates with the level of damage inflicted.

Early computational systems developed to segment comet assay cells were predominantly semi-automatic and relied heavily on thresholding-based methods, which made them highly dependent on maximum brightness pixel values (Helmma and Uhl, 2000; Ruz-Suarez et al., 2022). Subsequently, Gyori et al. (2014), introduced OpenComet, an automatic and freely available software system that employs adaptive thresholding to segment comets and identifies their heads based on intensity

* Corresponding author.

E-mail address: lavdie.rada@bau.edu.tr (L. Rada Ulgen).

<https://doi.org/10.51753/flsrt.1319546> Author contributions

Received 24 June 2023; Accepted 27 July 2023

Available online 26 August 2023

2718-062X © 2023 This is an open access article published by Dergipark under the [CC BY](https://creativecommons.org/licenses/by/4.0/) license.

profile analysis. However, this tool struggles to recognize overlapping and heavily damaged comets. In a similar vein, Lee et al. (2018), presented HiComet, a system that employs histogram thresholding for automatic comet cell segmentation, albeit without directly obtaining the segmentation of the comet's head (only head center and radius). Furthermore, this approach encounters difficulties in partitioning overlapping comets. Although these existing comet analysis systems have facilitated detection and segmentation to some extent, they rely on handcrafted image features, making them less effective in noisy backgrounds or when distinguishing individual cells within overlapped regions (Ruz-Suarez et al., 2022).

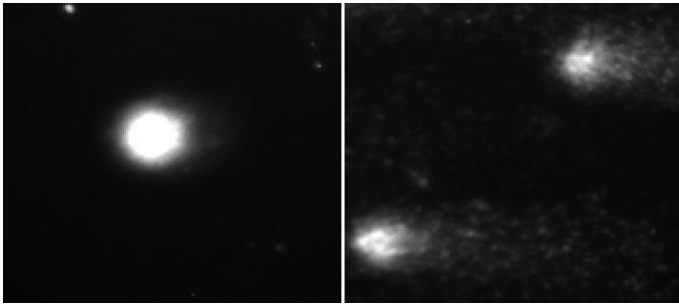


Fig. 1. Different imaging of comet assay cell with low level of DNA damage on the left and high level of DNA damage on the right.

The rapid advancement of machine learning and deep learning techniques has led to a shift in solving the segmentation of the comet assay, prioritizing these methods over fully exploring traditional image processing techniques. One of the first such methods was CometQ, proposed by Ganapathy et al. (2016), utilizes classical machine learning algorithms for the detection and quantification of DNA damage in comet assay images. Nevertheless, its segmentation results require a high amount of trained data, and unfortunately, the program is currently unavailable for download. This method was further followed by other works such as Afiahayati et al. (2022) proposed a CNN model for five-level classification of comet cells, adapting pre-processing image processing techniques and machine learning one. Similarly, Hafiyani et al. (2021), improved upon their previous work by incorporating a hybrid CNN and Extreme Learning Machine (ELM) method for comet classification on buccal mucosa cells, but manual interaction was still required. Lastly, Ruz-Suarez et al. (2022), proposed a system called U-NetComet, which is a fully convolutional neural network-based approach. The purpose of U-NetComet is to automate the segmentation of comets, reducing the need for user intervention and ensuring consistent and reproducible measurements. While the system can be regarded as state-of-the-art, comparable to other machine learning and deep learning algorithms mentioned earlier, its performance is dependent on a few factors. Firstly, it relies on a large and high-quality collection of trained data, which can be resource-intensive to gather. Additionally, tuning the hyperparameters of the system is crucial for optimal results, requiring careful optimization. Lastly, the system demands on machines with large memory capacity, which can limit its application in scenarios with limited resources (Taye, 2023).

In light of the limitations already known for machine learning and deep learning techniques, the author of this study believe that there is an unfilled gap that should be further investigated with the help of image processing techniques. This paper proposes a novel approach for comet segmentation by

utilizing dot enhancement-like structures, and adaptive histogram, which will improve image saturation, in combination with extended-maxima transform watershed segmentation to accurately identify the head and tail of comets, as well as extract essential cell properties for further analysis. The proposed system is a fully automated tool that can effectively segment individual cells in single-cell gel electrophoresis assay images.

The experiments are based on free available data taken from the website <https://www.clir-lab.org/u-netcomet> and some more data provided by Dr. Elda Pacheco-Pantoja from Mexico Medicine School, Health Sciences Division, Universidad Anahuac Mayab.

2. Materials and methods

2.1. Proposed method overall

The proposed method used two separate image processing algorithms to distinguish between comet heads and tails. The reason for such split is due to the fact that the head is a bright circular object whereas the tail is a fuzzy intensity spread in the surrounding of the head that easily can be mixed as a noise. The segmentation module determines whether each pixel belongs to the head or the tail of a comet. To easily follow the way the algorithm has been constructed readers can refer to the diagram of the model shown in Fig. 2.

The proposed identification and extraction of cells head comet assays combine a dot enhancement filter to distinguish and help in the detection of the head in each cell combined with simple threshold technique and refinement, which will avoid the low contrast circle-like structures of the background. Through experiments, it can be seen that the proposed algorithm it is robust compared to the other methods proposed in the literature and can detect hard cases where overlapping comets and heads, which are closed by, are observed and cannot be distinguished easily. The proposed method will mostly define accurately the head contours of such cases.

On the other hand, segmenting the tail of the comets is a real challenge and the existing method such as simple threshold, watershed, and region based would fail. In this work, a watershed segmentation technique based on an extended-maxima transform of the image is proposed, capable to capture corn-like structures, similar to how the tail of comets looks in general. The watershed segmentation based on the above idea might produce structures, which are part of the background. To refine it, segmented object that has a head as the center of the structure are considered.

The most challenging part of such work refers to nearby comets. In cases where nearby comets lack distinct boundaries, a distance function can be utilized to separate the tails. However, it is important to note that this approach may not provide high accuracy. Furthermore, obtaining opinions or expert input from specialists may be challenging due to the limited information available for such specific cases. The proposed system in this research provides a mathematical solution that depends on the circle-like property of the head of the comets.

The proposed algorithm provides two outputs: the original input image with additional contours, indicating the comet region and its head; and a file containing all the mathematical properties, such as head center, head and tail area, head and tail length, extracted from each segmented image.

2.2. Database

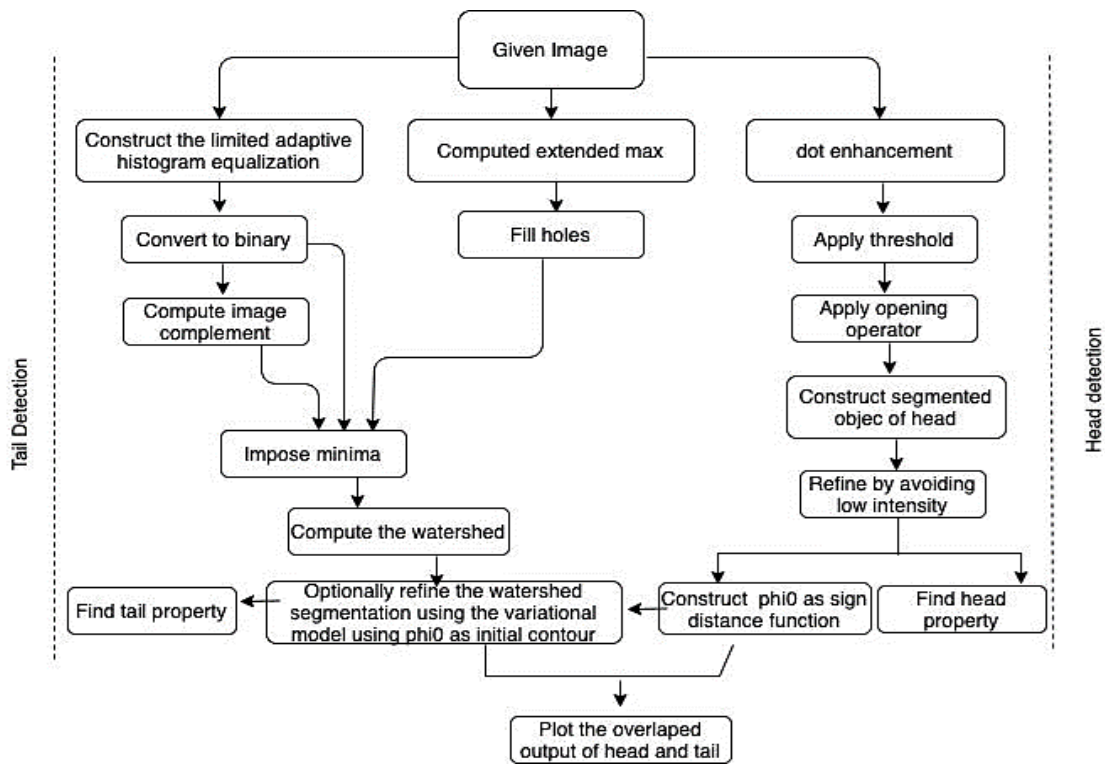


Fig. 2. The diagram of the proposed image processing system.

The initial data set comprises 140 grayscale images of comet assays, with a resolution of 1388×1038 pixels and 288×288 cropped from the original image size 1388×1038 . 1388×1038 pixels are original images taken from experiments whereas the 288×288 images are used for the training and validation of the UNetComets (2022) machine learning system application.

The small-size images have been provided as crop images by the specialist together with a boundary annotation. These images contain cells exhibiting varying degrees of damage, as well as different shapes and sizes due to the magnifying lens used (Fig. 3-9). The images in this research were processed as provided without any resizing or cropping as already used in

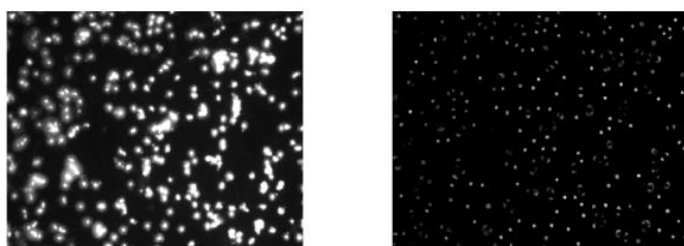


Fig. 3. Original image on left and dot enhanced image on the right.

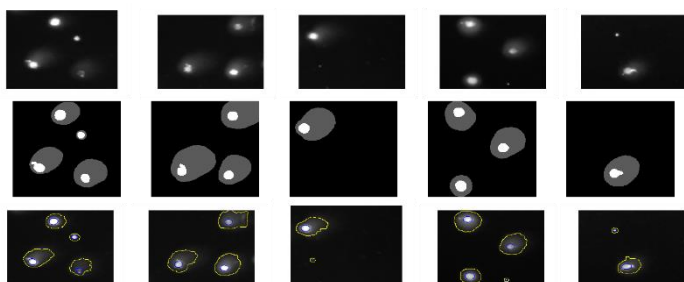


Fig. 4. Test of the proposed algorithm in cases where the comets are separated from each-other. The first row shows the original image, the second row the annotation of the head and the tail by experts and the last row the segmentation with the proposed algorithm.

machine learning techniques. The proposed algorithm can be further improved in the future to archive better accuracy but at this stage, it can be proved that there is no need for costly machine-learning techniques for such problems. Image processing can be a great alternative to solve them.

2.3. Comets head segmentation through dot enhancement filter

Dot enhancement filters are highly effective for circular-like structure detection; as is the segmentation of the assay images head; due to their ability to sensitively respond to dots while maintaining specificity by avoiding the generation of non-dot shapes. In difference with a simple threshold method based on the image intensity, the nearby comets, which are hard to be processed, can be split and as for the knowledge of the author, there is no such work that can properly segment such cases. The approach in this paper combines dot enhancement filters with a watershed-region-based segmentation technique segmentation for the tail of the comets. In this subsection, a concise overview of dot and line enhancement filters in the 2D domain is provided.

Dot and line enhancement filters operate by analyzing the eigenvalues of the 2D Hessian matrix at each location in the image space. Adopting the parameter-free techniques introduced acts as filter enhancement method. These techniques have shown improved sensitivity in nodule detection compared to previous methods. The output, denoted as $z(\lambda_1, \lambda_2)$, from the dot enhancement filters (or line enhancement filters) described in (Li et al., 2003), is obtained as the product of a magnitude function, g_{dot} (or g_{line} for line enhancement), and a likelihood function, k_{dot} (or k_{line} for line enhancement). In the following a brief explanation of these functions has been provided. Consider an image represented as $I(x, y)$, in a 2D domain, its second derivatives can be expressed as I_{xx} , I_{yy} , and I_{xy} . Now, let's assume that a line, denoted as $l(x, y)$, and a dot, denoted as $d(x, y)$, are fuzzy continuous shapes and second-order differentiable functions. The line $l(x, y)$ is oriented along the y-axis, allowing

any line parallel to the x-axis to be represented by a one-dimensional Gaussian function. On the other hand, the dot $d(x,y)$ is characterized by a fuzzy dot shape and can be represented by a 2D Gaussian function. Accordingly, a line and a dot can be described as follows:

$$l(x,y) = \exp\left\{-\frac{x^2}{2\sigma^2}\right\} \quad (1)$$

$$d(x,y) = \exp\left\{-\frac{x^2 + y^2}{2\sigma^2}\right\} \quad (2)$$

where σ the Gaussian parameter it determines the spread or width of the Gaussian function, indicating the size of the dot or the thickness of the line. For the center of a dot, the mixed second derivative I_{xy} is equal to zero. As a result, the dot enhancement filter relies solely on the two eigenvalues of the Hessian matrix namely λ_1 and λ_2 ;

$$\lambda_1 = K + \sqrt{K^2 - Q^2}, \lambda_2 = K - \sqrt{K^2 - Q^2}, \quad (3)$$

where $K = (I_{xx} + I_{yy})/2$, and $Q = I_{xx} I_{yy} - I_{xy} I_{yx}$. To maintain generality and without sacrificing its essence, making the assumption that λ_1 is the largest eigenvalue, satisfying the condition $|\lambda_1| \geq |\lambda_2|$. If this condition is not met, the values of λ_1 and λ_2 has been changed, making λ_1 the larger eigenvalue and λ_2 the smaller eigenvalue.

2.3.1. Construction of the likelihood functions, k_{dot} and k_{line}

The likelihood functions are directly associated with the sensitivity of indicating the probability that a pixel belongs to either a dot or a line. In order to enhance bright objects against a dark background, the sign of the second derivatives should be considered negative. Specifically, for a dot or a nodule-like object, one can anticipate that:

$$\lambda_1 \approx \lambda_2 = -1/\sigma^2 < 0. \quad (4)$$

The output $z(\lambda_1, \lambda_2)$ of the dot enhancement filters, as discussed in Li et al. (2003), is determined by the product of the magnitude function and the likelihood function. The likelihood of a dot can be defined as $e_2 = |\lambda_2|/|\lambda_1|$. Thus, the previously mentioned conditions (4) can be expressed in the following manner:

$$\begin{aligned} \text{dot: } k_{dot}(\lambda_1, \lambda_2) &= e_2 = |\lambda_2|/|\lambda_1|, \\ \text{line: } k_{line}(\lambda_1, \lambda_2) &= 1 - e_2 = (|\lambda_1| - |\lambda_2|)/|\lambda_1|. \end{aligned}$$

Each of the two likelihood functions produces an output value of 1 for a particular shape and an output value of 0 for the other shape.

2.3.2. Construction of the magnitude functions, g_{dot} and g_{line}

For the dot enhancement filter, a suitable choice for the magnitude function is to utilize the value of λ_2 . This is because λ_2 yields a value greater than 0 for a dot and a value of 0 for a line. Therefore, one can define the magnitude function for the dot enhancement filter as $g_{dot} = |\lambda_2|$. Similarly, for the line enhancement filter, the magnitude function can be defined as $g_{line} = |\lambda_1|$. This choice allows us to obtain a value greater than 0 for a line and a value of 0 for a dot. By incorporating the two fundamental criteria of sensitivity and specificity, one can

achieve a high-quality output for the enhanced filter.

$$z_{dot}(\lambda_1, \lambda_2) = \begin{cases} |\lambda_2|^2/|\lambda_1| & \text{for } \lambda_1 < 0, \lambda_2 < 0 \\ 0 & \text{otherwise.} \end{cases} \quad (5)$$

$$z_{line}(\lambda_1, \lambda_2) = \begin{cases} |\lambda_1| - |\lambda_2| & \text{for } \lambda_1 < 0, \lambda_2 < 0 \\ 0 & \text{otherwise.} \end{cases} \quad (6)$$

To fully utilize the filter described in equations (5) and (6), it is beneficial to consider the influence of noise and the scale of objects, which necessitates a multiscale enhancement approach. In order to enhance objects across a range of scales $[d_0, d_1]$, a two-step process can be followed. First, a Gaussian smoothing filter is applied within the scale range of $[d_0/4, d_1/4]$. Subsequently, the dot enhancement filter, as described earlier, is applied, following the methodology outlined in Li et al. (2003) and Lindeberg (1998). This combination of Gaussian smoothing and dot enhancement filters enables the effective enhancement of objects at various scales, taking into account both noise reduction and object scale considerations. The enhancement filters involve two steps that need to be repeated N times, with each repetition increasing the smoothing scale. This repetition helps generate N-enhanced images with progressively smoother scales. The selection of N discrete smoothing scales can be determined using the following approach: $\sigma_1 = d_0/4, \sigma_2 = r\sigma_1, \dots, \sigma_N = r^{N-1}\sigma_1 = d_1/4$, where $r = (d_1/d_0)^{1/(N-1)}$. To obtain the final output and enhance or extract features at multiple scales in an image the maximum value from the N individual filters has been selected. This approach allows us to achieve a dot-enhanced structure and suppress lines-looking structure, see Fig. 3. The dot enhancement image provides boundaries of all the heads as a threshold operator is applied. On the other side, as the dot enhancement operator does not depend on the image intensity to about circle-like structures which are not part of the foreground, the image intensity inside the boundaries of the obtained objects was considered and then refine the head output by avoiding low-intensity circle-like structures. After the refinement, all the properties of the segmented heads, such as perimeters, center, area, etc., has been found. On the other hand, the segmented image of the heads can be used as an initial level set for the next step where a variational model optionally is applied to refine the watershed segmentation output of the comet's tail.

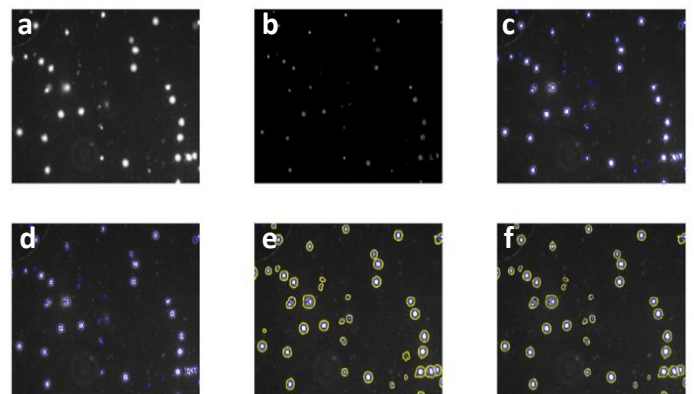


Fig. 5. Comet assay dataset samples from the original size image without cropping as commonly would be used for machine learning techniques. (a) Original image, (b) Dot enhanced image, (c) Threshold of the dot enhanced image, (d) Head center detection, (e) Segmentation of the tail, (f) Final output after refinement.

In order to proceed and get the second level of segmentation; involving the information of the tail; a standard

threshold for the obtained image followed by an opening operator with a disc structuring element of radius 3 has been used. In this way, in the case of nearby comets, one will be able to have some information on each of them separately.

2.4. Comets tail segmentation through an extended-maxima transform watershed segmentation

To perform the segmentation of the tail detection for each head, a multi-level segmentation algorithm, inspired by the work of Qin et al. (2013) and Rada et al. (2014), has been employed. The work of Rada et al. (2014), accurately delineates and separate the detected spines, circular-like structures from the background and other structures present in the image, whereas the work of Qin et al. (2013), separates the touching corn kernels used in the watershed segmentation into individual segments by enabling better analysis and measurement of each kernel. In difference with this work, the minima between the extended-maxima transform of the image and the background has been imposed. To achieve this, the extended-maxima transform of the image and the background is computed.

It is important to note that in general, the watershed algorithm tends to produce larger boundaries than the actual boundaries in case of the presence of noise. Therefore, to achieve accurate segmentation of the tail regions, a variational-based algorithm can be employed to refine the edges. This can be easily decided by the user as he evaluated the noise range of the given data.

2.4.1. Extended-maxima transform

The extended-maxima transform as a variation of the H-maxima transform in mathematical morphology is shortly summarized in the following: The H-maxima transform is used to suppress pixels above a certain intensity and extract local maxima related to target objects from a grayscale image. The Extended-Maxima Transform can calculate the regional maximum and create a binary image. In the H-maxima transformation, all maxima whose depth (intensity) is below or equal to a given threshold h are suppressed. This is achieved by performing the reconstruction of the grayscale image f from $f - h$ using dilation. Mathematically, the $HMAX_h(f)$ is defined as:

$$HMAX_h(f) = R_f^{\delta}(f - h),$$

where f represents the grayscale of the original image and h is the threshold value.

The Extended-Maxima Transform, denoted as $EMAX_h(f)$, is minima of the corresponding H-maxima transformation, which is obtained by applying regional maximum:

$$EMAX_h(f) = RMAX[H, MAX_h(f)].$$

In order to label the segments obtained from the watershed algorithm as either part of the comet assay or not, the information of the center of each comet head obtained from the previous step over the binary image has been used. Moreover, to get better information on the range of the intensity of the comet's tail, for each watershed segment image intensity of the region without the intensity of the head already segmented in the previous step has been considered. This will allow the evolution of the refinement of the variational model to find the largest region where the tail takes place.

2.4.2. Optional refinement with geodesic active contour model

In this approach, the variational function combines an edge detection function inspired by the Le Guyader and Gout (2008) approach with a region-based function similar to the Chan-Vese (CV) model proposed by Chan and Vese (2001). The level-set formulation of this variational function can be expressed as:

$$\delta_{\epsilon}(\phi(x)) \left\{ \mu \nabla \cdot \left(g(x) \frac{\nabla \phi(x)}{|\nabla \phi(x)|} \right) - \lambda ((I(x) - c_1)^2 - (I(x) - c_2)^2) \right\} = 0,$$

with μ and λ constants, $g(x)$ an edge detection image, c_1 and c_2 are the mean intensity of the image foreground and background, respectively, computed as follows:

$$g(x) = \frac{1}{1 + |\nabla I(x)|^2} \quad c_1 = \frac{\int_{\Omega} f(x) H_{\epsilon}(\phi(x))}{\int_{\Omega} H_{\epsilon}(\phi(x))} \quad c_2 = \frac{\int_{\Omega} f(x) (1 - H_{\epsilon}(\phi(x)))}{\int_{\Omega} (1 - H_{\epsilon}(\phi(x)))} dx$$

where H_{ϵ} and δ_{ϵ} represent the regularized Heaviside and the corresponding Delta function, respectively, that guarantee the derivation continuity at perpendicular jumps. In this paper, the approximation for the Heaviside and delta function is given as:

$$H_{\epsilon} = \frac{1}{2} \left(1 + \frac{\delta}{\pi} \arctan\left(\frac{x}{\epsilon}\right) \right) \quad \text{and} \quad \delta_{\epsilon} = \frac{d}{dt} H_{\epsilon}(x) = \frac{\epsilon}{\pi(\epsilon^2 + x^2)}$$

while as the first initial level set ϕ_0 it is a distance function obtained from the binary image of the head segmentation.

3. Results and discussion

In this section, the results of the output experiments that showcase the performance of the proposed comet segmentation and property extraction algorithm has been shown. Demonstrating the effectiveness of the proposed algorithm and its segmentation accuracy has been first shown. The experiments were run over the dataset provided by free available from the website <https://www.clir-lab.org/u-netcomet> and some new data by Dr. Elda Pacheco-Pantoja from Mexico Medicine School, Health Sciences Division, Universidad Anahuac Mayab. To evaluate the proposed approach, the obtained results were compared with those obtained from existing noncommercial software OpenComet (Gyori et al., 2014), and UNetComet (Ruz-Suarez et al., 2022).

The primary objective of this study is to detect heads of comets with an already-known diameter ranging from 4(d0) to 32(d1). To achieve this, dot filters with varying smoothing scales, ranging from 1 to 8, were applied across all of the experiments. The dilation and opening operator uses a standard disk structuring element size 3. The threshold used while applying the imposed minima between the extended-maxima transform of the image and the background has a value of 40. In case the variational model will be activated for the refinement, the parameters used are set to specific values: $\mu = 500$, $\lambda = 1$, and $\epsilon = 1$. The optimization of these parameters is a subject for future work and remains to be explored. Fig. 4 depicts a successful segmentation of a head and the tail of different images taken from the set of 288×288 images, achieved through the dot-enhancement-based comets-dissemble technique. The accuracy of the proposed segmentation algorithm was assessed by comparing its results with manual delineations provided by a domain expert. To measure the similarity between the

algorithm's output and the manual delineations, the Dice coefficient, as introduced by Dice et al. in 1945, has been employed. Dice coefficient ranges from 0 to 1, with 1 indicating a perfect match. After evaluating 40 different comets, their respective Dice coefficients were calculated. On average, the algorithm achieved a Dice coefficient of 0.843, with a minimum value of 0.671 and a maximum value of 0.986. The results show a high segmentation accuracy, with the algorithm closely matching the expert manual delineations.

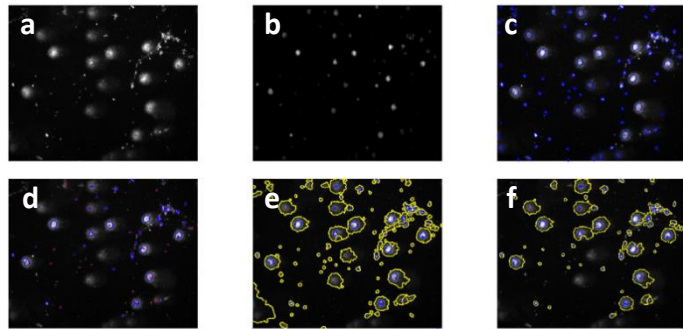


Fig. 6. Second example of comet assay dataset samples from the original size image without cropping as commonly would be used for machine learning techniques. (a) Original image, (b) Dot enhanced image, (c) Threshold of the dot-enhanced image, (d) Head center detection, (e) Segmentation of the tail, (f) Final output after refinement.

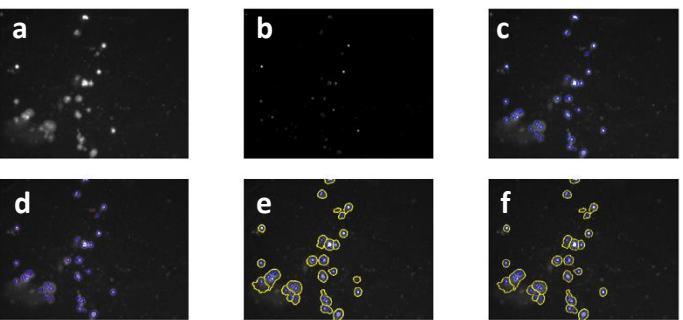


Fig. 7. Third example of comet assay dataset samples from the original size image without cropping as commonly would be used for machine learning techniques. (a) Original image, (b) Dot enhanced image, (c) Threshold of the dot-enhanced image, (d) Head center detection, (e) Segmentation of the tail, (f) Final output after refinement.

Fig. 5 - 7 are showcases of the qualitative segmentation outputs obtained by the proposed model during the validation phase. The samples are the originally taken images without cropping as commonly would be used for machine learning techniques. It can be observed that pixels for the head and the tail of the comets are classified accurately. All those figures provide examples demonstrating the successful partitioning of two overlapping comets which other methods will fail as shown in the following. In all the figures the original image (a), dot enhancement output (b) followed by the head segmentation, and head center detection (d), which will play a role in the refinement of the tails as part of a comet or not, tail segmentation using extended-maxima transform watershed segmentation (e), and the last figure showing the accurate segmentation of the tail and head of comets has been shown.

It can be easily seen from those figures that the proposed model does not have difficulty running with a high accuracy in each of the images. The time to process each image is at most 20 seconds per image.

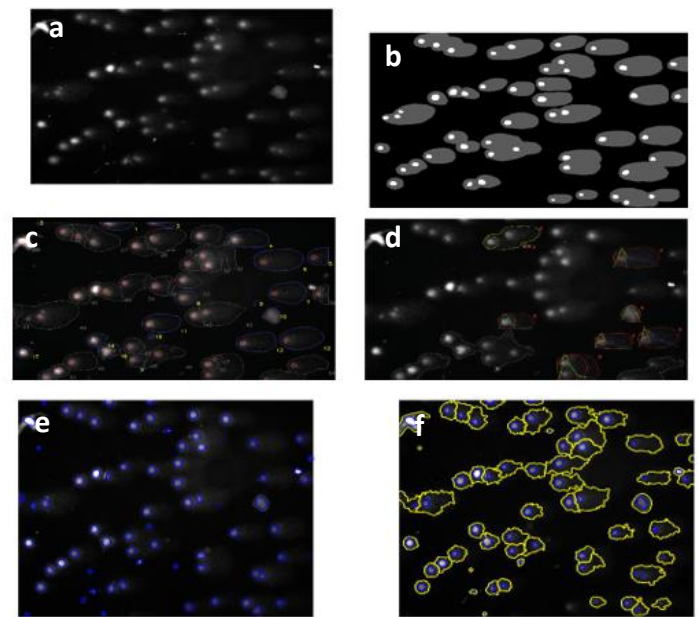


Fig. 8. Comet assay dataset samples from the original size image. (a) Original image, (b) Annotated image by experts, (c) UnetComet segmentation, (d) OpenComet segmentation, (e) Head segmentation with the proposed model, (f) Final output of the proposed model.

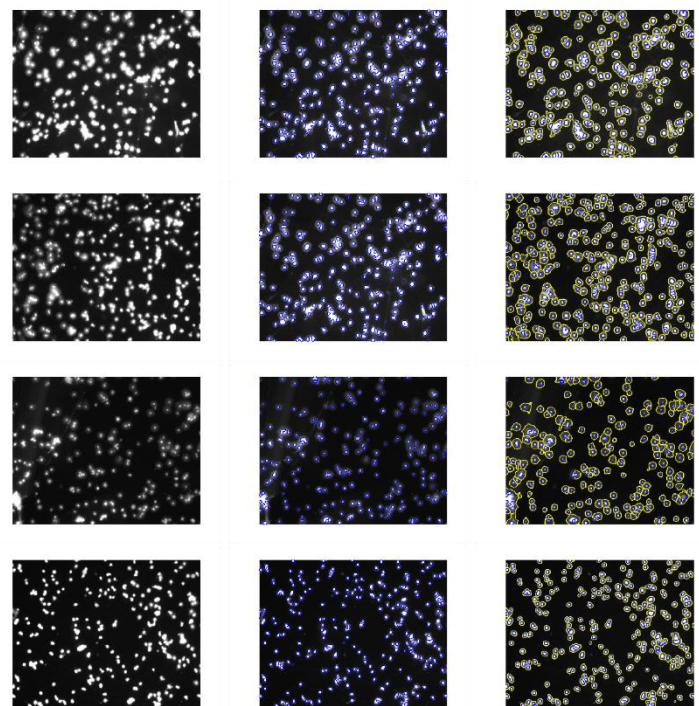


Fig. 9. Successful segmentation of comet heads and tails for superimposed comets.

To evaluate the performance of the proposed algorithm, comparison experiments were conducted against a state-of-the-art system called OpenComet (Gyori et al., 2014), and UNetComet (Ruz-Suarez et al., 2022).

In order to compare the segmentation results of both systems in comparison with the proposed algorithm, hard cases, with images that safer from low quality as well as merged comets, were considered. The objective of this process is to identify the estimated boundaries of superimposed comets and separate them into individual comets.

As it can be observed from Fig. 8 segmentation results obtained from both systems fail in a high-accuracy segmentation. The OpenComet system shows low performance whereas though the UnetComet performs relatively well one can see that UnetComet will over-segment objects such as comets number 45, 47, and 50 in Fig. 8 (c). Similar to this example UnetComet will over-segment or miss to segment comets in cases as shown in Fig. 9.

As part of this study, extremely hard cases, where not only superimposed comets appear as part of the images but at the same time the image is of low quality due to distortion, were considered.

As shown in Fig. 10 the proposed algorithm is not successful. This is going to be a motivation for the future work where dehazing and deblurring techniques can be hired for such cases as an image preprocessing technique.

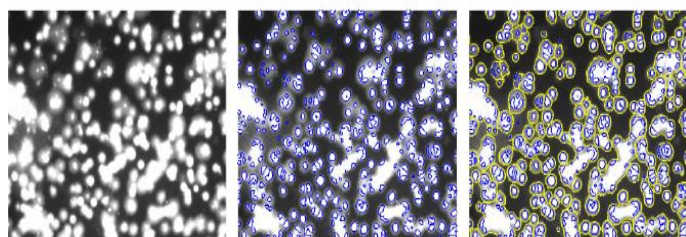


Fig. 10. Fail of the proposed system top be considered as future work.

References

- Afiyahayati A. E., Yanuarieska R. D., & Mulyana, S. (2022). GamaComet: A deep learning-based tool for the detection and classification of DNA damage from buccal mucosa comet assay images. *Diagnostics (Basel)*, 12(8), 2002.
- Chan, T. F., & Vese, L. A. (2001). Active contours without edges. *IEEE Transactions on Image Processing*, 10, 266-277.
- Chatterjee, N., & Walker, G. C. (2017). Mechanisms of DNA damage, repair, and mutagenesis. *Environmental and Molecular Mutagenesis*, 58(5), 235-263.
- Dice, L. R. (1945). Measures of the amount of ecologic association between species. *Ecology*, 26, 297-302.
- Fairbairn, D. W., Olive, P. L., & O'Neill, K. L. (1995). The comet assay: a comprehensive review. *Mutation Research/Reviews in Genetic Toxicology*, 339, 37-59.
- Ganapathy, S., Muraleedharan, A., Sathidevi, P. S., Chand, P., & Rajkumar, R. P. (2016). CometQ: An automated tool for the detection and quantification of DNA damage using comet assay image analysis. *Computer Methods and Programs in Biomedicine*, 133, 143-154.
- Le Guyader, C., & Gout, C. (2008). Geodesic active contour under geometrical conditions: Theory and 3D applications. *Numerical algorithms*, 48, 105-133.
- Gyori, B. M., Venkatachalam, G., Thiagarajan, P., Hsu, D., & Clement, M. V. (2014). OpenComet: An automated tool for comet assay image analysis. *Redox Biology*, 2, 457-465.
- Hafiyani, Y. T., Yanuarieska, R. D., Anarossi, E., Sutanto, V. M., Triyanto, J., & Sakakibara, Y. (2021). A hybrid convolutional neural network-extreme learning machine with augmented dataset for DNA damage classification using comet assay from buccal mucosa sample. *International Journal of Innovative Computing, Information and Control*, 17(4), 1191-11201.
- Helmma, C., & Uhl, M. (2000). A public domain image-analysis program for the single-cell gel-electrophoresis (comet) assay. *Mutagenesis*, 466, 9-15.
- Lee, T., Lee, S., Sim, W. Y., Jung, Y. M., Han, S., Won, J. H., ... & Yoon, S. (2018). HiComet: a high-throughput comet analysis tool for large-scale DNA damage assessment. *BioMed Central Bioinformatics*, 19(1), 49-61.
- Li, Q., Sone, S., & Doi, K. (2003). Selective enhancement filters for nodules, vessels, and airway walls in two-and three-dimensional CT scans. *Medical Physics*, 30, 2040-2051.
- Lindeberg, T. (1998). Feature detection with automatic scale selection. *International Journal of Computer Vision*, 30, 77-116.
- Ostling, O., & Johanson, K. (1984). Microelectrophoretic study of radiation-induced DNA damages in individual mammalian cells. *Biochemical and Biophysical Research Communications*, 123, 291-298.
- Qin, Y., Wang, W., Liu, W., & Yuan, N. (2013). Extended-maxima transform watershed segmentation algorithm for touching corn kernels. *Advances in Mechanical Engineering*, 5, 268046.
- Rada, L., Erdil, E., Argunsah, A. O., Unay, D., & Cetin, M. (2014). Automatic dendritic spine detection using multiscale dot enhancement filters and sift features. *2014 IEEE International Conference on Image Processing (ICIP)*, Paris, France, 26-30.
- Ruz-Suarez, D., Martin-Gonzalez, A., Brito-Loeza, C., & Pacheco-Pantoja, E. L. (2022). Convolutional neural network for segmentation of single cell gel electrophoresis assay. In: Brito-Loeza C., Martin-Gonzalez A., Castañeda-Zeman V., Safi A. (eds) *International Symposium on Intelligent Computing Systems* (pp. 57-68). Cham: Springer International Publishing.
- Singh, N. P., McCoy, M. T., Tice, R. R., & Schneider, E. L. (1988). A simple technique for quantitation of low levels of DNA damage in individual cells. *Experimental Cell Research*, 175(1), 184-191.
- Taye, M. M. (2023). Understanding of machine learning with deep learning: architectures, workflow, applications and future directions. *Computers*, 12(5), 91.
- Uthirapathy, S. (2023). Cytostatic effects of avocado oil using single-cell gel electrophoresis (comet assay). *Aro-The Scientific Journal of Koya University*, 11(1), 16-21.

Cite as: Rada Ulgen, L. (2023). Automated comet assay segmentation using combined dot enhancement filters and extended-maxima transform watershed segmentation. *Front Life Sci RT*, 4(2), 92-98.

4. Conclusion

This research introduces a simple image process system designed for the segmentation of head and tail comet assay cells. It utilizes a dot enhancement filter as the main success for the head segmentation and an extended-maxima transform watershed segmentation for the segmentation of the tail. The proposed system serves as an efficient computer-assisted biomedical tool, offering a promising solution for the segmentation task in comet assay experiments. Moreover, its success opens up possibilities for easy implementation.

Acknowledgement: The author of this work extend her heartfelt appreciation to Dr. Elda Pacheco-Pantoja from the School of Medicine, Health Sciences Division, Universidad Anahuac Mayab, Mexico, for generously providing extended database to the one already found on the website <https://www.clir-lab.org/unetcomet>. Her valuable comments have greatly enhanced the quality and depth of this study.

Conflict of interest: The author declares that he has no conflict of interests.

Informed consent: The author declares that this manuscript did not involve human or animal participants and informed consent was not collected.